*Biomedical & Pharmacology Journal*, September 2025. Vol. **18**(3), p. 1962-1974

# Candesartan Polymeric Microneedle Arrays: Design, Optimization, and Characterization Made with a 3D Fused Deposition Method

**Ola Ali Tarawneh[1]*, Yahia Fayiz Makableh[2], Ala Abdul Kareem Alhusban[1], Ahmad Mustafa Malkawi[2], Anas Mutawa Alhusban[2], Alghadeer Haider Al-Shammari[1] and Mohammad Majed Hailat[1]**

[1]Pharmacy Department, Al-Zaytoonah University of Jordan, Amman, Jordan.
[2]Department of Nanotechnology, Jordan University of Science and Technology, Irbid, Jordan.
*Corresponding Author E-mail: drolatarawneh@hotmail.com

https://dx.doi.org/10.13005/bpj/3229

(Received: 28 March 2025; accepted: 18 August 2025)

**Microneedle arrays are a simple, noninvasive transdermal delivery system. The technique's preparation, optimization, and scaling up are all active research topics. This paper investigates a simple method for making microneedle molds for inverted-solvent casting preparation of microneedle arrays. The effect of different resins and printing conditions on the geometry of microneedle arrays was investigated using stereolithography 3D printing. Four molds prepared in this study were selected to be filled with candesartan cilexetil in a mixture of polymers that include EMPROVE® and gantrez. The fully formed MNAs were evaluated based on skin perforation, drug release through Franz cells, bending ability, and sterilization. The model drug and the resultant MNAs were evaluated based on the MNA's shape, drug release, and compression resistance. To improve process quality and achieve highly aligned defect-free needles, the surface of the fabricated microneedles was modified with a monolayer of hyaluronic acid. The structure design was optimized using computer-aided design. The molds were tested by producing candesartan cilexetil microneedle array patches for transdermal delivery. This study discovered that hot plate post-treatment and avoiding shear force during mold peeling are critical for fabricating high-quality arrays. Candesartan cilexetil microneedles were successfully prepared, and the release rate was 73.36 ± 7.29% of the loaded candesartan cilexetil amount over 24 hours. The obtained molds can potentially be used to fabricate microneedle arrays successfully.**

**Keywords:** Candesartan Cilexetil; 3D printer; Fused Deposition; Hyaluronic Acid; Microneedle Arrays; Mold.

Microneedles arrays (MNAs) patches are emerging as a promising transdermal drug delivery system.[1] MNAs are small, painless, and minimally invasive arrays, usually less than millimeters long. They deliver drugs throughout the skin by penetrating the outermost layer, the stratum corneum. [2,3] This approach provides merits over traditional medication delivery methods, including injections, oral tablets, and transdermal patches. Small chemicals, peptides, proteins, and vaccines may be delivered using MNAs.[4] Microneedles arrays are expected to increase patient compliance and treatment effectiveness.[5] The market for transdermal patches, including MNAs, has expanded dramatically in recent years. By 2025, the transdermal medication delivery

market is anticipated to reach a value of around 95.77 billion US Dollars.[6]

There are several methods used for the fabrication of MNAs. Each MNA fabrication method has advantages and limitations, and the choice of a certain technique for design and fabrication depends on the specific application requirements and the desired properties of the microneedles.[7] For example, MNAs may be produced using solvent casting in an inverted mold that requires a precise fabrication of molds. However, the potential expense of manufacturing molds and the challenge of mass production are some of this method's main drawbacks.[8] Laser ablation is another technique for creating microscopic needles from a substrate using lasers. However, being a time-consuming process and unsuitable for mass production are the main downsides.[9] Etching, which utilizes chemicals to remove material from a substrate in a targeted manner employed to fabricate MNAs, still provides low accuracy and homogeneity in needle shape.[10]

Moreover, drawing lithography, which employs a fine-tipped pen to trace microneedles onto a substrate, has demonstrated difficulty achieving consistent needle shape and high manufacturing throughput.[11] Besides, making a microneedle mold, filling it with a polymer solution, and cementing it is known as solvent casting. This method's limitations include the need for great accuracy and homogeneity in the needle's shape, which can make it difficult to accomplish the intended functions of these structures, and the solvent employed could be poisonous or bad for the skin.[12] However, a recent method for MNA fabrication is the 3D printing of molds, which utilizes additive manufacturing techniques to create microneedles layer by layer. The process of scaling up MNA manufacturing has several challenges. However, this technique offers better flexibility and can be scaled up, even though achieving high resolution and mechanical strength can be difficult.[13] Candesartan (an ARB) effectively lowers blood pressure in hypertension, significantly reduces heart failure morbidity and mortality (fewer hospitalizations and deaths), and slows diabetic nephropathy progression through renal protective effects [14–16], could be effectively delivered through transdermal methods, overcoming challenges like skin penetration and absorption variability, using noninvasive technology.[17,18]

The purpose of this study is to prepare a novel application of stereolithography (SLA) 3D printing for MNA fabrication, study the effects of different resins and printing conditions on needle geometry, and the preparation of microneedles in the designated molds to produce candesartan cilexetil microneedle array patches for transdermal delivery. In addition, hydrophilic hyaluronic acid coating to fill microneedles without requiring a centrifuge is novel in this research and could lead to increased production of commercial microneedles on a larger commercial scale.

## MATERIALS AND METHODS

### Materials

Rigid 10k, Elastic 80A, standard black resins, and general-use silicon molds were obtained from Form Labs (USA). Hyaluronic acid, candesartan cilexetil, Emprove® 5-88, dimethyl sulfoxide (DMSO), and methanol were obtained from Merck (Germany). Gantrez s-97 was kindly donated from Ashland (Ireland). PVP k30 was purchased from BBC Chemicals. All chemicals were used as received without any further purification.

### Experimental Procedure and used apparatus

The fabrication of a mold that can be used to cast biocompatible materials to make dissolving microneedles was performed by using the SLA 3D printing technique. Three different types of resins were selected for this study, including Rigid 10k, Elastic 80A, and Standard black. Formlabs Form 3L printer (Massachusetts, USA) was used for 3D printing of the test structures. Different layers' widths and printing angles were used for each specimen. After printing the molds, the fabricated structures were removed from the printer and washed with Isopropyl alcohol, and then cured with UV-light in a curing machine (AMS Technologies, Bayern, Germany) to maximize material properties and to achieve the curing point of each different types of used resin. The printed structures were evaluated for their dimensional accuracy and surface quality using a Quanta FIG 450 Scanning Electron Microscope (SEM) (Thermofisher, Massachusetts, USA), a Profilm 3D optical

profilometer (California, USA), and an OKN177 Reflective light microscope (Kern optics, Balingen, Germany).

**CAD Design and Mesh Analysis**

To achieve accurate and precise printing conditions, using microneedles in 3D printing necessitates a correct tiny mesh in the CAD program. Fusion 360 software was utilized in this investigation to prepare the different MNAs designs to be printed. Initially, the automated mesh feature incorporated into Fusion 360 did not give the necessary degree of detail for microneedle printing. Inadequate mesh density resulted in gaps or bulges in the printed sample, hampered its operation. To address this issue, the mesh was manually modified to fine meshing level, resulting in high-quality printing with no bulging or gaps. As a result, while configuring the mesh settings in the CAD program for micro-needle printing, it is critical to consider the printing material's size and the needed degree of detail of the printed MNAs. Figure 1 shows the meshing analysis of the MNA's CAD designs.

**MNAs preparation and characterization**

**Fabrication of CC MNAs microneedles**

To prepare the microneedle-loaded drug, a mixture of 30% w/v Emprove® in distilled water, 10%w/v PVP, and 1% gantries s-97 in a volumetric ratio of 3:6:1 were mixed properly. Then, 16 mg of candesartan was dissolved in 1 mL methanol with two drops of dimethylsulfoxide (DMSO) and vortexed until a clear solution was obtained. Afterward, 450 µL was taken from the resultant mixture and mixed properly with 150 µL of the candesartan solution in an Eppendorf, then injected slowly in the in-house customized 3D-printed microneedles. The molds were tapped gently and then left to dry for 48 hours. The microneedles were peeled and evaluated based on their full formation. The dimensions of the successful microneedle formulation's tips were measured using ImageJ software.[19]

**Insertion test**

The penetration efficiency of the fabricated microneedles was tested using rat skin. The study was implemented using experimental procedures approved by the Al-Zaytoonah University animal ethics committee (Ethics Number: 01/08/2022-2023). The rats' skin in this study was carefully shaved using a scalpel blade, and the fat layer underneath the hypodermis layer was removed. The tissue samples were frozen at "80 °C and naturally thawed before the tests. The microneedles were pressed manually for 1 minute, and images were taken using a digital microscope.[20]

**Drug release and diffusion of CC microneedles through Franz cells**

Phosphate buffer saline solution (pH 7.4) was prepared by adding 2.86g $NaH_2PO_4$, 0.2g $KH_2PO_4$, and 8g NaCl in 1L of distilled water. The drug release experiment was conducted with modifications.[20,21] Three excised rat skin sheets were mounted on 3 Franz diffusion cells (PremeGear, USA) (the exposed area was 1X1 cm to be fitted with the surface area of the chamber, average weight was 31.03 mg), and it was assured that the exposed area of the upper part of the shaved skin is facing the donor chamber, where then the microneedles patch was pressed on the top part of the skin for 60 sec. The receiver chambers were filled with 8 mL phosphate buffer saline (pH=7.4) to provide adequate skin hydration. The cells were incubated at 37 ± 0.5°C under occlusive conditions for 24 h with stirring at 60 rpm.

At predetermined intervals, 8/ mL samples were withdrawn from the receptor chamber via the side arm using a long syringe and immediately replaced with fresh PBS to maintain sink conditions. The withdrawn samples were filtered using a 0.45/ µm PVDF syringe filter (chosen for its low protein binding and compatibility with organic solvents) to remove particulate matter. The filtrate was analyzed for candesartan content using UV–visible spectrophotometry at 255/ nm (Shimadzu UV 1800, Japan). Cumulative drug release was expressed as mean/ ±/ SD.

**Mechanical features of the fabricated microneedles: Compression**

The ability of the microtips to bend and resist fracture was measured using TA.XT Plus texture analyzer (Stable Microsystem, Surrey, UK) [22]. The images of microneedle tips were captured using a polarized microscope and then measured via ImageJ software. The microneedles were later compressed using a flat probe with a diameter of 7mm. The flat probe was applied on the surface of the tips of the microneedles and left in contact for 30 sec at 40 N as compression force. Subsequently, the images were taken, and the height reduction was analyzed using ImageJ. The reduction in

microneedle height was recorded as a percentage reduction compared to the original height.[19,22]

**Sterilization of the fabricated microneedles**

The CC-fabricated microneedles were subjected to sterilization by two methods; the first one was autoclaving for 10 minutes, and the second method was using a UV lamp. The microneedles were fixed on an agar Petri dish, sterilized with UV Lamp, and left in an incubator for 24 h at 37°C to check microbial growth. At 24 h, the Petri dish was removed from the incubator and checked for the presence or absence of microbial growth. As a control, an agar plate was sterilized and placed in the incubator, and images of the agar Petri dishes were acquired.

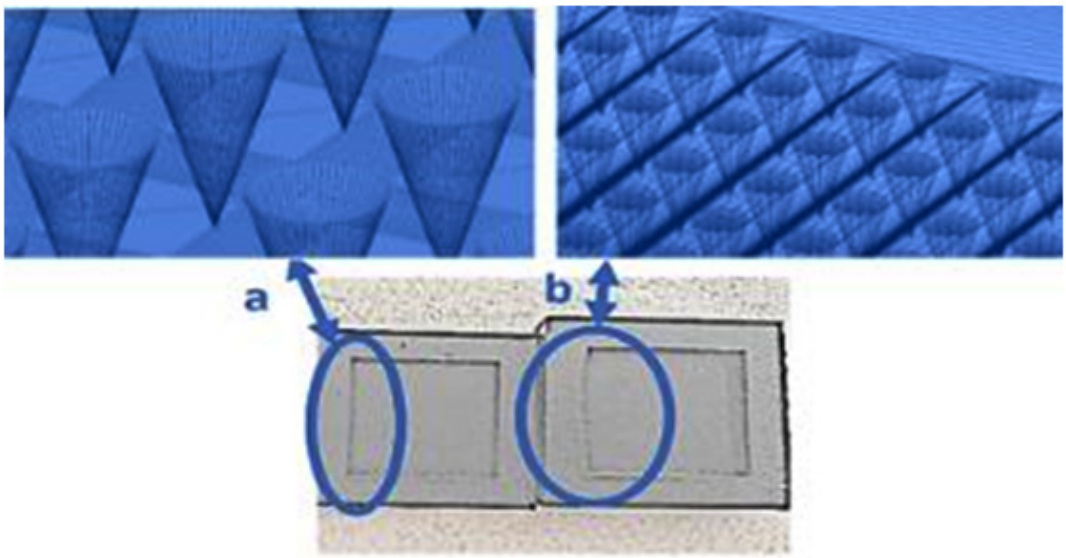


**Fig. 1.** (a) Proper meshing effect on sample uniformity, (b) Sample distortion due to poor mesh formation

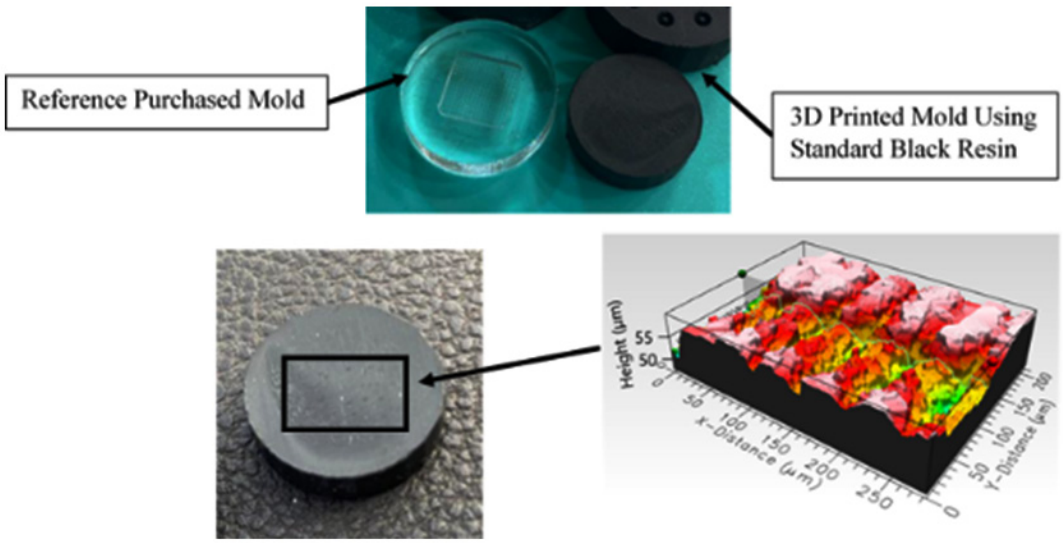


**Fig. 2.** Optical profiler images for standard black resin mold 50 ìm x 50 ìm base and 150 ìm height at a 0° printing angle

## RESULTS

Several features must be addressed and optimized to properly employ SLA for 3D printing of the microneedles, such as material properties, CAD design, printing resolution, curing time, and post-processing techniques. However, when these factors are controlled, the SLA technique has the potential to revolutionize microneedle manufacture. The SLA approach enables the fabrication of intricate structures and patterns that would be impossible to achieve with conventional microneedle manufacturing technologies. It also enables rapid prototyping and design iteration, leading to faster development and optimization of microneedles for a wide range of applications. Notwithstanding the difficulty in regulating the parameters, the SLA technique is a viable choice for producing novel and effective microneedle-based technologies.

### Direct/Indirect Mold 3D Printing Results

Commercially available silicon molds, with dimensions of 50 ìm square pyramid base and 150 ìm height, were purchased to reference the 3D printed molds using the SLA technique. Directly printing MNAs molds with the same dimensions showed poor printing quality, as seen in the optical profiler image illustrated in Figure 2.

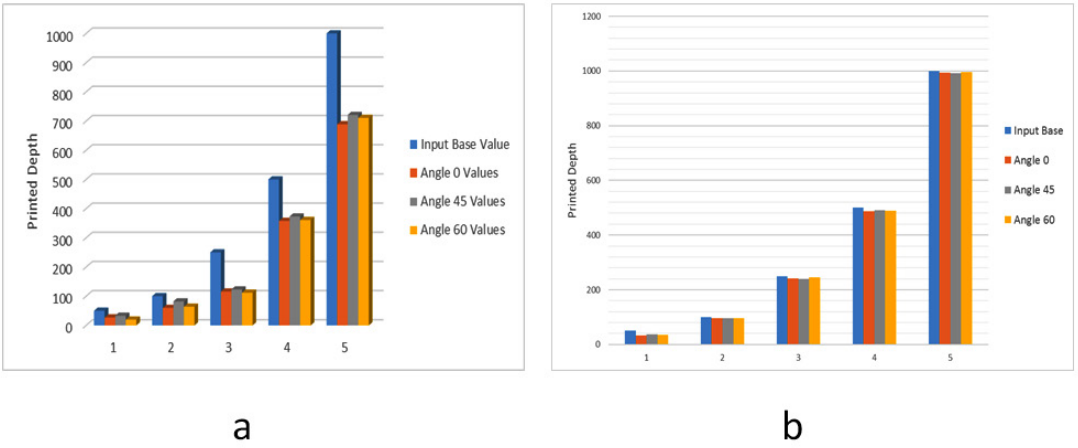


**Fig. 3.** Performed analysis on the printed MNAs: a) Degree of error between input and output values for direct molds MNAs at different printing angles, and b) Degree of error between input and output values for positively extruded MNAs at different printing angles

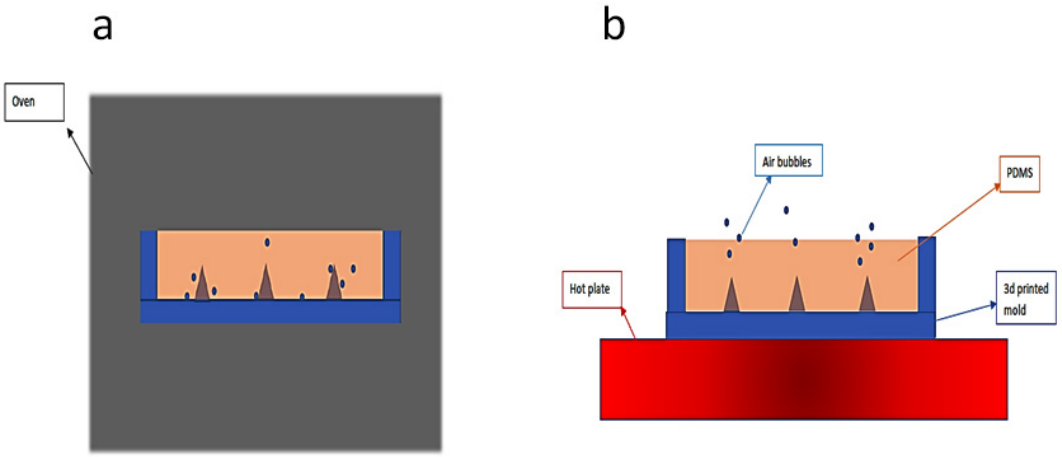


**Fig. 4.** An illustration of the bubble formation when curing PDMS uses a) a conventional oven and b) a hot plate

Further analysis was conducted to check the possibility of printing direct molds. Square pyramid needles with an aspect ratio (AR) of 2.5 and depth of (50 ìm, 100 ìm, 250 ìm, 500 ìm, and 1000 ìm, respectively) were printed and examined to check the accuracy of the printing. Results were gathered in Figure 3 (a). The resin used for this test was the Flexible 80A, and the layer height was set to 100 ìm. In order to overcome the rubbery (flexibility) property of the Flexible 80A, it was decided to print the needles first and then prepare a silicon master mold from the printed MNAs. Positive extruded square pyramid needles were also tested under the same conditions as the direct mold needles. AR of 2.5 and depths of (50 ìm, 100 ìm, 250 ìm, 500 ìm, and 1000 ìm, respectively) were

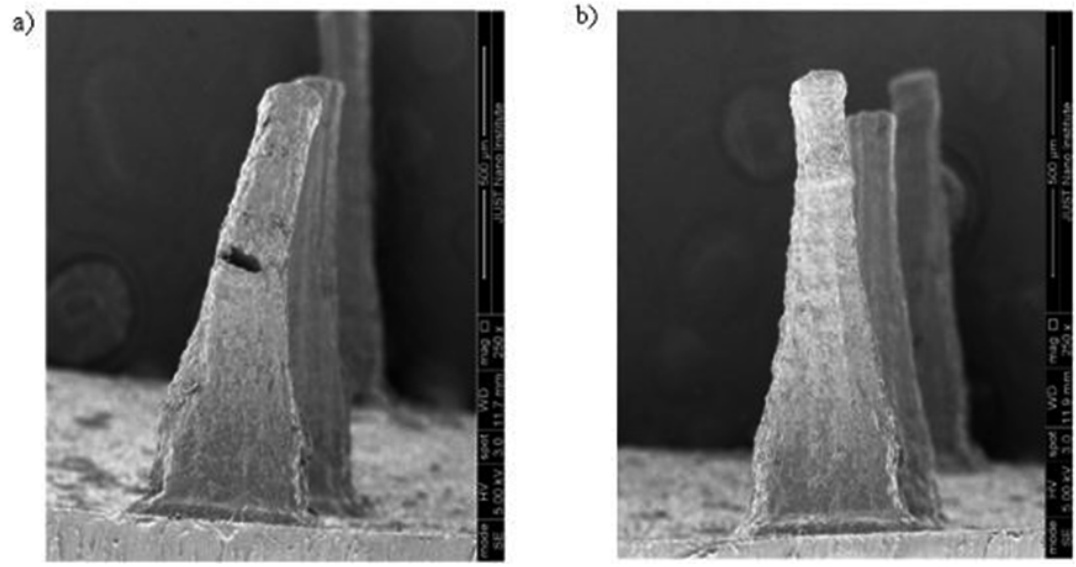


**Fig. 5.** SEM images of the rigid 10k needles after PDMS peeling a) sample without hyaluronic acid monolayer coating, and b) sample with hyaluronic acid monolayer coating

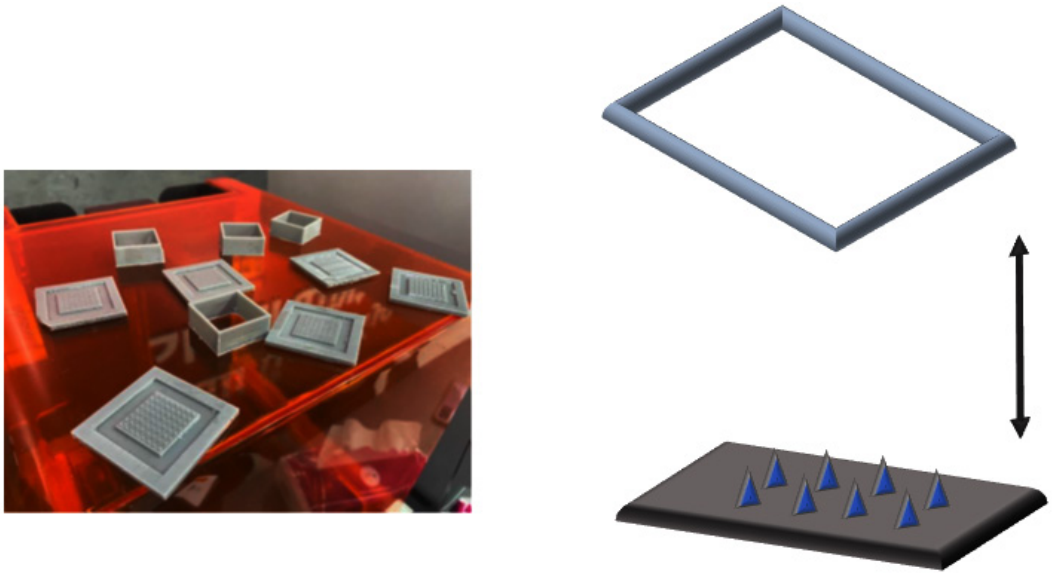

**Fig. 6.** An image showing the optimum master mold peeling direction

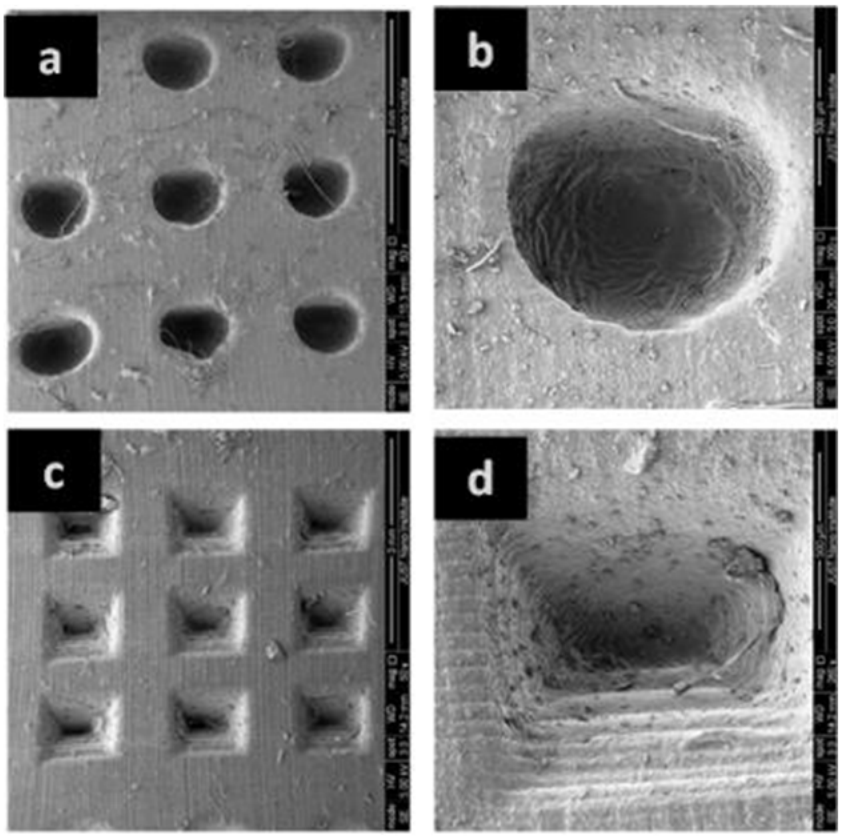


**Fig. 7.** SEM images of the prepared structures (a, b) Conical MNAs base deformation after 3D printing with standard black resin 100 ìm layer width (c, d) Square pyramid MNAs shape deformation

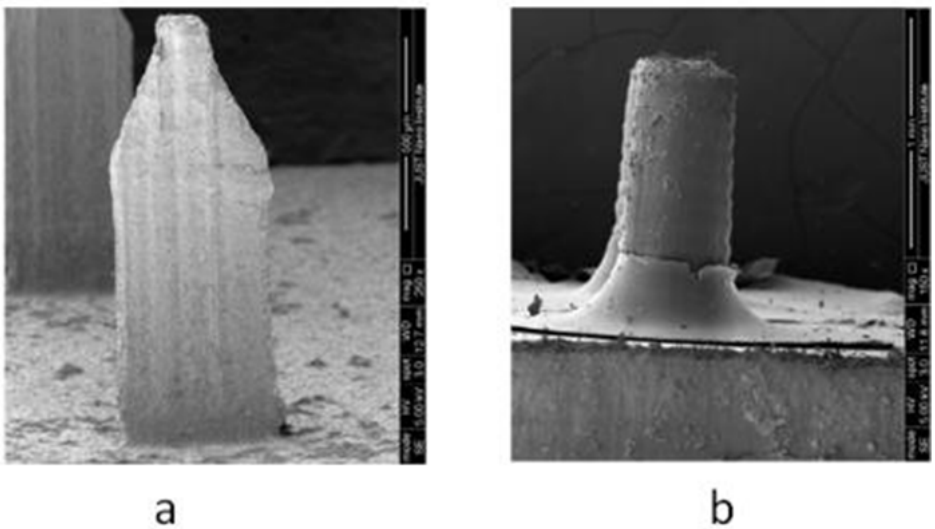


**Fig. 8.** SEM images of the spear and b cylindrical MNAs after 3D printing with standard black resin, with a 100 ìm layer width Microneedles

printed using Flexible 80A resin, and the layer height was set to 100 ìm. The obtained analysis is shown in Figure 3 (b).

**Post-treatment process results**

After processing the 3D printing of the microneedles, the printed structures were ready for silicon mold casting using polydimethylsiloxane (PDMS). It was noticed that curing the PDMS in an oven is a faster approach but results in lower quality molds when compared to curing on a hot plate, as bubbles tend to escape more easily on a hot plate and result in a more accurate master mold. Tests were performed at 80 °C temperature. This process is illustrated in Figure 4.

**Resin-PDMS Interaction**

The resin can interact with the PDMS in three different ways: the first one is the resin and PDMS strong adhesion, the second one is resin inhibiting the curing of PDMS, and the third one is resin and PDMS weak adhesion. Since easy peeling of the master mold from the 3D printed piece is important, the most desirable case is the third case, where resin and PDMS show weak adhesion. This type of interaction was mostly seen in the standard black resin. The rigid 10k resin also showed good PDMS curing, but unlike the standard black resin, it showed a strong adhesion with the PDMS. The last resin tested was the elastic 80A resin. This resin prevented the curing of the PDMS substantially. Even with a high curing agent concentration and temperatures, the PDMS in the elastic 80A resin never cured, making it unsuitable for microneedle fabrication.

An approach that can be used to reduce the adhesion between the rigid 10k resin and PDMS to increase the quality of the final needles is to coat the PDMS mold with a hydrophobic surface of hyaluronic acid by using Langmuir-Blodgett (LB) technique. The LB technique is widely used for preparing thin films of hydrophobic and hydrophilic materials on various surfaces.[23] Two MNA structures were printed using the rigid 10k resin and cast using PDMS. One of the samples was coated with a monolayer of hyaluronic acid by the LB technique. To make the hyaluronic acid surface hydrophobic, fatty acid, a hydrophobic molecule, was introduced into the monolayer. SEM Images for the Rigid 10k needles after PDMS peeling were taken for both samples, as shown in Figure 5.

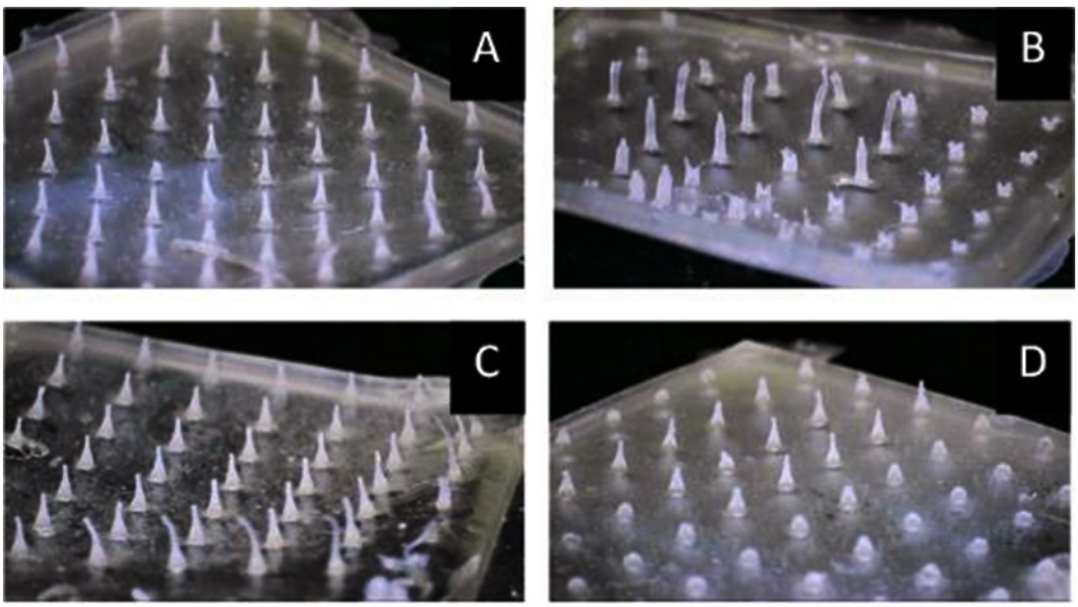


**Fig. 9.** showing the candesartan loaded microneedles, where A illustrates fully formed microneedles fabricated in 3D printed mold after silicon curing at 80°C on hotplate overnight, B illustrates the microneedles poured in 3D printed mold where the silicone curing took three h in an oven at 180°C, C shows microneedles in 3D printed microneedles where the silicon curing was at 80°C in an oven overnight. D represents microneedles formed in 3D-printed microneedles where silicone curing was at 110°C for 1.5 hours on a hotplate

It is also vital that the PDMS peeling process be perpendicular to the needle direction to prevent any shear stress that may form. This was obtained when the walls of the sample were printed separately to be able to peel them vertically, as illustrated in Figure 6.

**Shape deformation results**

Following 3D printing, the resulting sample undergoes a phenomenon whereby its geometric properties are altered due to its minuscule scale. As evidenced by the images below, the shapes intended to be perfect squares with dimensions of 500 ìm x 500 ìm and perfect circles with a diameter of 500 ìm are subjected to deformations. The deformation of the printed object can be attributed to various factors, including the manufacturing process itself, as well as environmental conditions, such as temperature and humidity. Therefore, it is crucial to consider these factors when producing and handling 3D-printed objects, particularly those intended for precision applications. The SEM images of these structures are shown in Figure 7.

In addition to the square above and circular shapes, other MNAs' geometries, including spear-shaped and cylindrical microneedles, were also investigated. These shapes also exhibited slight deformations following 3D printing, which can be attributed to the nature of the additive manufacturing process. 3D printing works by depositing layers of material, one on top of the other, which can lead to small variations in the shape and size of the final product. These findings highlight the importance of understanding the

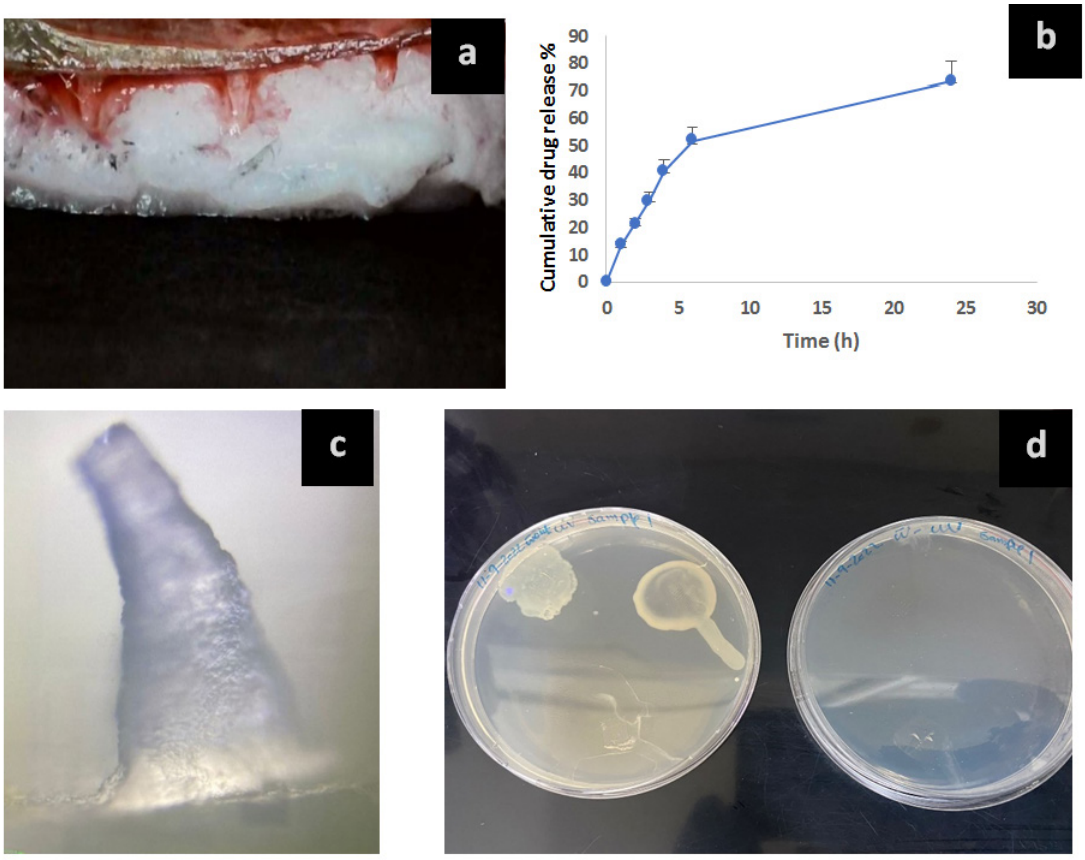


**Fig. 10.** a: Image of rat skin showing the prepared microneedles penetration of the skin. b: Candesartan release from MNA showing release over 24 hours from the microneedle's arrays showing 73.36± 7.29%. The release best fits the Korsmeyer-Peppas model because it has the highest $r^2$ value. c; Microneedles tip subjected to 40N compression force applied through TA texture analyzer probe (1000 X magnification of polarized microscope) d) The sterilization of prepared candesartan cilexetil microneedle by autoclave showing no growth (left) versus control (right). Note: Microneedles dissolved, and their traces appeared on the agar gel.

limitations of 3D printing technology when designing and producing microneedles, as slight deformations can impact their functionality and effectiveness. Hence, the geometry plays an important role in producing MNAs. **Figure 8**. shows the SEM images of the spear and cylindrical MNAs.

A desired process produces a better MNA shape post-treatment using a hot plate. In addition, proper meshing and printing angles are needed to reduce shape deformations to a minimum. Moreover, coating the MNAs with a monolayer of hyaluronic acid has a positive effect on help keeping the MNA's structures undeformed during the peeling process.

**Fabrication of microneedles**

The full formation was observed in the mold presented in Figure 9, A, where the tips of the microneedles appear pyramidal and pointed, as this mold was fabricated using the hotplate at 80 C overnight. The height of the tips was analyzed using ImageJ and was found to be 1064.17±26.99 µm. Figure 9, B shows either broken or long microneedle tips prepared in the mold fabricated in an oven at 180 C for 3 hr. Figure 9, C presents an incomplete formation, and the tips appear curved as its mold was fabricated using the oven at 80 C overnight. Figure 9, D shows no formation of microneedles as its mold was fabricated using the hotplate at 110 C for 1.5 hr. Based on the successful formation of the designated microneedles in the mold shown in Figure 9 A, it was considered for further characterization.

**Insertion**

The successful candesartan cilexetil microneedles were obtained from the mold cured in a hotplate at 80æ%C (Figure 9A). Hence, the designated microneedles were subjected to further characterization. The essential characterization test was to prove the microneedles' ability to penetrate the skin. In this way, the microneedles were colored and pressed against the skin of rats, as illustrated in Figure 10a. The microneedles successfully penetrated the stratum corneum and viable epidermis, suggesting strong potential for transdermal drug delivery via intradermal microchannels [24].

**Diffusion/Drug release and skin deposition**

The diffusion of microneedles of candesartan cilexetil was conducted in Franz's cell. The cumulative diffused drug after 24 h was found to be 73.36± 7.29%, whereas the amount in the skin after it was extracted was found to be 24.36±5.35%. Figure 10b indicates that the drug was deposited in the skin after 24 hours.

**Compression**

Compression measures the ability of the microneedles to bend when exposed to applied force over surface area. Bending was clear in the tips (Figure 10c illustrates a polarized microscope image of the bent tip). The average length of the microneedle tips was calculated and found to be 1.0641±26.99mm. However, after compression with 40 N force, the reduction in height was found to be 0.541mm. Therefore, the reduction in percentage was 49.00%. It is worth mentioning that the bend was also noticed in the experiment and imaging of skin penetration, as observed in Figure 10a.

**Sterilization**

The autoclave made the gel melt immediately and thus was deemed unsuitable as a sterilization technique. However, the UV lamp showed an adequate noninvasive approach for sterilization. The microneedles were not affected. However, water in the agar dish and the incubator's warmth led to the melting of the micro-microneedles. Upon comparison of the microneedles Petri dish (right) versus the control Pe-tri dish (Figure 10 d, left panel), it is clear that no microbial growth was detected on the microneedles, and thus, it was deemed more appropriate for the sterilization of the fast dissolving microneedles. There are contrary reports on the need to sterilize microneedles. However, it was decided to sterile the produced microneedle as the method was deemed noninvasive, rapid, and effective. The microneedle looks melted due to the interaction between the microneedle polymer and water from the agar medium.

## DISCUSSION

The present study demonstrated the feasibility of using Stereolithography (SLA) 3D printing technology to design and fabricate microneedle arrays with optimized geometries. To fabricate optimized microneedle arrays using SLA printing, it is essential to have a proper mesh in the CAD software to ensure accurate and precise

geometry. It is also important to note that the master mold cannot be printed directly; the microneedles should be printed individually to create a silicon master mold. Post-treatment of the microneedles is also necessary to improve their quality, and a hotplate was found to offer merit over conventional ovens attributed to the ability of the formed air bubbles to escape, resulting in a better-quality product. The interaction between the resin and PDMS can lead to sticking, which was addressed by coating the PDMS with a hydrophobic surface and peeling the mold perpendicular to the surface. The lifespan of the resin is limited, and continuous use and proper storage are essential to maintain its quality.

Furthermore, it should be noted that the 3D printing process can result in shape deformations, and different shapes exhibit varying degrees of deformation. Therefore, it is crucial to understand the limitations and potential solutions to the microneedle's fabrication process. Despite the limitations of SLA printing technology for microneedle fabrication, it is still a potential technique for revolutionizing the field of microneedle drug delivery systems. Once the limitations are fully understood and overcome, SLA printing can provide a cost-effective, customizable, and scalable method for producing microneedle arrays with optimized geometries. This would allow for tailored drug delivery to specific patient needs and improved precision and accuracy in clinical applications. With continued advancements in SLA printing technology and further research to understand and overcome, the potential for this technology to impact healthcare and medicine is immense. In doing so, the microneedles treated in the hotplate were fabricated from water-soluble polymers, which are Emprove® 5-88, gantrez s-97, and PVP K30. Emprove® 5-88 is a high molecular weight PVA polymer with a degree of hydrolysis of 88% that can be used in drug delivery. Gantrez s-97 was reported to improve the stability of MNAs and enhance the shelf life. PVP was used alone or with different polymers to treat diseases and skin conditions like melasma, psoriasis, and rheumatoid arthritis. The combination of the three polymers showed nicely formed MNAs, and we could load CC, a class II drug, after it was treated with DMSO and ethanol to enhance its solubility in the mixture. The mold treated in the hotplate for three hours (Figure 10A) produced the optimum MNAs tested for its ability to penetrate the rats' skin, as observed in Figure 10 a.

Furthermore, although the drug is poorly soluble in water, the technology of dissolving microneedles enabled it to release over 76% of the loaded amount. The release fits the Korsmeyer-Peppas model most since it has the highest $r^2$ value. The remaining amount in the skin necessitates adding chemicals or physical aid to enhance the full diffusion of the drug so it will not accumulate on the skin and lead to skin irritation over chronic use, as CC is typically prescribed for chronic diseases. The sterility of MNAs is a factor considered in this study, as the MNAs were assumed to penetrate the skin and thus may be a source of contamination. Our results showed that UV lamp sterilization was adequate to sterile the MNAs, and as such, they can be safely employed in the treatment.

The results obtained from the mold design using 3D printing technologies and the fabrication of CC-loaded MNAs show potential in continuing the research in this field and employing those technologies in transdermal drug delivery.

## CONCLUSION

This study presents a comprehensive evaluation of candesartan polymeric microneedle arrays prepared using a 3D fused deposition technique, demonstrating its efficacy in addressing key challenges such as avoiding shear force during mold peeling which is critical for fabricating high-quality arrays. Through rigorous experimental analysis and comparative performance assessments, the proposed approach has proven to enhance candesartan cilexetil microneedles preparation, outperforming existing state-of-the-art methods. The findings underscore the potential of this framework to contribute significantly to biomedical engineering, drug delivery, dermatology, and materials science, offering practical implications for real-world deployment and further research. Future work may explore the integration of the prepared MNs for human treatment and apply it on human to further advance the capabilities and robustness of the proposed methodology. Overall, this study lays a solid foundation for ongoing innovation in drug delivery, fostering more intelligent, efficient, and adaptable solutions.

## ACKNOWLEDGMENT

The authors would like to express their sincere gratitude to Al-Zaytoonah University of Jordan, School of Pharmacy, for providing the facilities and support necessary to carry out this work. Special thanks are extended to the faculty members and technical staff of the School of Pharmacy for their valuable assistance, guidance, and encouragement throughout the study. The authors also acknowledge the contributions of colleagues and students who offered constructive discussions and technical help during different stages of this research.

**Funding Source**

This research was funded by the Scientific Research and Innovation Support Fund Grant Number (MPH/1/17/2018), and the Deanship of Scientific Research at Jordan University of Science and Technology and Deanship of Scientific Research at Al-Zaytoonah University of Jordan.

**Conflict of Interest**

The author(s) do not have any conflict of interest.

**Data Availability Statement**

This statement does not apply to this article.

**Ethics statement**

Institutional Review Board Statement: The study was implemented using experimental procedures approved by Al-Zaytoonah University of Animal Ethics Committee (Ethics Number/ protocol code: 01/08/2022-2023).

**Informed Consent Statement**

This study did not involve human participants, and therefore, informed consent was not required.

**Clinical Trial Registration**

This research does not involve any clinical trials.

**Permission to reproduce material from other sources**

Not Applicable.

**Authors' Contribution**

Ola Tarawneh: Conceptualization, Methodology, Writing – Original Draft, Supervision, Project Administration; Yahia F. Makableh: Data Collection, Analysis, Writing – Review & Editing; Ala. A. Alhusban: Visualization, Supervision, Project Administration; Ahmad Malkawi: Data Collection, Analysis; Anas Alhusban: Data Collection, Analysis, Writing – Review & Editing; Alghadeer Al-Shammari: Methodology, Data Collection; Mohammad Hailat: Conceptualization, Methodology, Writing – Review & Editing.

## REFERENCES

1. Kulkarni D, Gadade D, Chapaitkar N, et al. Polymeric Microneedles: An Emerging Paradigm for Advanced Biomedical Applications. *Sci Pharm*. 2023;91(2). doi:10.3390/scipharm91020027
2. Gupta J, Gill HS, Andrews SN, Prausnitz MR. Kinetics of skin resealing after insertion of microneedles in human subjects. *Journal of Controlled Release*. 2011;154(2):148-155. doi:10.1016/j.jconrel.2011.05.021
3. Haq MI, Smith E, John DN, et al. Clinical administration of microneedles: Skin puncture, pain and sensation. *Biomed Microdevices*. 2009;11(1):35-47. doi:10.1007/s10544-008-9208-1
4. Jahan N, Archie SR, Shoyaib A Al, Kabir N, Cheung K. Recent approaches for solid dose vaccine delivery. *Sci Pharm*. 2019;87(4). doi:10.3390/scipharm87040027
5. Dharadhar S, Majumdar A, Dhoble S, Patravale V. Microneedles for transdermal drug delivery: a systematic review. *Drug Dev Ind Pharm*. 2019;45(2):188-201. doi:10.1080/03639045.2018.1539497
6. Richter-Johnson J, Kumar P, Choonara YE, du Toit LC, Pillay V. Therapeutic applications and pharmacoeconomics of microneedle technology. *Expert Rev Pharmacoecon Outcomes Res*. 2018;18(4):359-369. doi:10.1080/14737167.2018.1485100
7. Rad ZF, Prewett PD, Davies GJ. An overview of microneedle applications, materials, and fabrication methods. *Beilstein Journal of Nanotechnology 12:77*. 2021;12(1):1034-1046. doi:10.3762/BJNANO.12.77
8. Kuo SC, Chou Y. A Novel Polymer Microneedle Arrays and PDMS Micromolding Technique. *Journal of Applied Science and Engineering*. 2004;7(2):95-98. doi:10.6180/JASE.2004.7.2.08
9. Evens T, Malek O, Castagne S, Seveno D, Van Bael A. A novel method for producing solid polymer microneedles using laser ablated moulds in an injection moulding process. *Manuf Lett*. 2020;24:29-32. doi:10.1016/J.MFGLET.2020.03.009
10. Wilke N, Mulcahy A, Ye SR, Morrissey A. Process optimization and characterization of

silicon microneedles fabricated by wet etch technology. *Microelectronics J*. 2005;36(7):650-656. doi:10.1016/J.MEJO.2005.04.044

11. Lee K, Jung H. Drawing lithography for microneedles: A review of fundamentals and biomedical applications. *Biomaterials*. 2012;33(30):7309-7326. doi:10.1016/J.BIOMATERIALS.2012.06.065
12. Mansoor I, Liu Y, Häfeli UO, Stoeber B. Arrays of hollow out-of-plane microneedles made by metal electrodeposition onto solvent cast conductive polymer structures. *Journal of Micromechanics and Microengineering*. 2013;23(8):085011. doi:10.1088/0960-1317/23/8/085011
13. Economidou SN, Douroumis D. 3D printing as a transformative tool for microneedle systems: Recent advances, manufacturing considerations and market potential. *Adv Drug Deliv Rev*. 2021;173:60-69. doi:10.1016/J.ADDR.2021.03.007
14. Zhang Z, Yang H, Guo H. Comparative efficacy and safety of six angiotensin II receptor blockers in hypertensive patients: a network meta-analysis. *Int J Clin Pharm*. 2024;46(5):1034-1043. doi:10.1007/S11096-024-01755-5,
15. Young JB, Dunlap ME, Pfeffer MA, et al. Mortality and morbidity reduction with candesartan in patients with chronic heart failure and left ventricular systolic dysfunction: Results of the CHARM low-left ventricular ejection fraction trials. *Circulation*. 2004;110(17):2618-2626. doi:10.1161/01.CIR.0000146819.43235.A9,
16. KDIGO 2022 Clinical Practice Guideline for Diabetes Management in Chronic Kidney Disease kidney I N T E R N A T I O N A L. Accessed August 6, 2025. www.kidney-international.org
17. Ali HH, Hussein AA. Oral nanoemulsions of candesartan cilexetil: formulation, characterization and in vitro drug release studies. *AAPS Open*. 2017;3(1). doi:10.1186/s41120-017-0016-7
18. Sharma K, Mittal A, Agrahari P. *Skin Permeation of Candesartan Cilexetil from Transdermal Patch Containing Aloe Vera Gel as Penetration Enhancer*. Vol 10.; 2016.
19. Schneider CA, Rasband WS, Eliceiri KW. NIH Image to ImageJ: 25 years of image analysis. *Nat Methods*. 2012;9(7):671-675. doi:10.1038/nmeth.2089
20. Ebrahiminejad V, Faraji Rad Z. Design, Development, and Testing of Polymeric Microblades: A Novel Design of Microneedles for Biomedical Applications. *Adv Mater Interfaces*. 2022;9(29). doi:10.1002/admi.202201115
21. Mahmoud NN, Alkilany AM, Dietrich D, Karst U, Al-Bakri AG, Khalil EA. Preferential accumulation of gold nanorods into human skin hair follicles: Effect of nanoparticle surface chemistry. *J Colloid Interface Sci*. 2017;503:95-102. doi:10.1016/j.jcis.2017.05.011
22. Larrañeta E, Moore J, Vicente-Pérez EM, et al. A proposed model membrane and test method for microneedle insertion studies. *Int J Pharm*. 2014;472(1-2):65-73. doi:10.1016/j.ijpharm.2014.05.042
23. Oliveira ON, Caseli L, Ariga K. The Past and the Future of Langmuir and Langmuir-Blodgett Films. *Chem Rev*. 2022;122(6):6459-6513. doi:10.1021/ACS.CHEMREV.1C00754/ASSET/IMAGES/MEDIUM/CR1C00754_0047.GIF
24. Meiser SL, Pielenhofer J, Hartmann AK, et al. Microneedle-enhanced drug delivery: fabrication, characterization, and insights into release and permeation of nanocrystalline imiquimod. *Frontiers in Drug Delivery*. 2024;4:1425144. doi:10.3389/FDDEV.2024.1425144/BIBTEX